Princeton Plasma Physics Laboratory

PPPL- 4539

PPPL- 4539

High Accuracy Wavelength Calibration For A Scanning Visible Spectrometer

Filippo Scotti and Ronald Bell

July, 2010

Prepared for the U.S. Department of Energy under Contract DE-AC02-09CH11466.

Princeton Plasma Physics Laboratory
Report Disclaimers

Full Legal Disclaimer

Trademark Disclaimer

PPPL Report Availability

Princeton Plasma Physics Laboratory:

http://www.pppl.gov/techreports.cfm

Office of Scientific and Technical Information (OSTI):

http://www.osti.gov/bridge

Related Links:

U.S. Department of Energy

Office of Scientific and Technical Information

Fusion Links

High accuracy wavelength calibration for a scanning visible spectrometer[a)]

Filippo Scotti[b)] and Ronald E. Bell
Princeton Plasma Physics Laboratory, Princeton, New Jersey 08543, USA

Spectroscopic applications for plasma velocity measurements often require wavelength accuracies ≤ 0.2 Å. An automated calibration for a scanning spectrometer has been developed to achieve a high wavelength accuracy over the visible spectrum, stable over time and environmental conditions, without the need to recalibrate after each grating movement. This method fits all relevant spectrometer parameters using multiple calibration spectra. With a stepping-motor controlled sine-drive, accuracies of $\sim$0.025 Å have been demonstrated. With the addition of a high resolution (0.075 arcsec) optical encoder on the grating stage, greater precision ($\sim$0.005 Å) is possible, allowing absolute velocity measurements within $\sim$0.3 km/s. This level of precision requires monitoring of atmospheric temperature and pressure and of grating bulk temperature to correct for changes in the refractive index of air and the groove density, respectively.

I. INTRODUCTION

A spectroscopic system with a high wavelength accuracy is required by many applications such as line identification and plasma velocity measurements. While a fixed wavelength spectrometer can sustain an accurate calibration, typical commercial scanning spectrometers have a wavelength uncertainty of $\sim$1 Å after the grating is moved. A recalibration is required at each new spectral range. In order to preserve scanning capabilities and a high wavelength accuracy, different approaches have been attempted by several groups: among these, automated inter-discharge recalibration procedures[1] and permanent dedication of a few optical fibers for wavelength calibration by means of a calibration lamp[2]. High accuracy calibrations across the detector have also been tried using one or a few spectra to try to fit the spectrometer parameters. With this approach, wavelength accuracies of the order of 0.03 Å have been achieved across the mid-plane of a detector if at least one measurement of a spectral line is made to determine the diffraction angle to a sufficient accuracy each time the grating is moved[3]. The ability to predict wavelengths without relying on frequent recalibrations or the knowledge of at least one line position would be extremely advantageous in a scanning spectrometer. This would require a high precision positioning system for the grating (or an independent measurement of the grating angle), a high accuracy calibration over the whole spectrum, and stability in the alignment and calibration with time and changes in atmospheric conditions.

In this paper, two calibration methods are presented for a scanning visible spectrometer on a 2D detector. Although the calibrations are presented for a particular lens based spectrometer, they can be applied in principle to any scanning spectrometer. The first method relies on a stepping motor controlled sine drive (or any grating positioning system); the use of multiple spectra from a neon lamp allows the fitting of all the grating equation parameters. Limiting this approach is the large number of parameters to be fit and the resolution and reproducibility of the grating positioning that determines the final achievable wavelength accuracy. The second calibration method utilizes the same setup but with the addition of an optical encoder, capable of accuracies of the order of 0.075 arcsec in angle measurements. The grating angle is thereby determined without relying on the positioning reproducibility of the stepping motor.

The high accuracies needed in this process require the monitoring and correction of other environmental parameters, such as air temperature and pressure and the grating bulk temperature. Necessary controls and alignment procedures will also be presented.

II. EXPERIMENTAL SETUP

For the work described in this paper a prototype, lens-based, visible scanning spectrometer was used. Details of the spectrometer are described elsewhere[4] but the components relevant to the work described in this paper are briefly illustrated in the next two paragraphs.

Two lenses were used as focusing and collimating optics. A diffraction grating (2160 grooves/mm) with a BK7 glass substrate was mounted on a rotary table. A stepping motor (1.58 μm per step) was used to control a sine drive for the grating positioning. For testing purposes, an 8 bit CMOS sensor (1280×1024, 5.2 μm per pixel) was employed as the detector. A thermocouple was used to measure the grating bulk temperature while a thermometer and a barometer were used to monitor air pressure and temperature. A movable slit system was developed in order to correct for the chromatic aberrations of the lenses[4]. The second calibration method to be presented, relies additionally on a high accuracy optical encoder, used to independently measure the grating angle with an accuracy of 0.075 arcsec[5].

The whole system was operated by a single Visual Basic program controlling the stepping motor, the slit adjustment, temperature and pressure measurements, en-

[a)] Contributed paper, published as part of the Proceedings of the 18th Topical Conference on High-Temperature Plasma Diagnostics, Wildwood, New Jersey, USA, May 2010.
[b)] fscotti@pppl.gov

coder reading and spectroscopic data acquisition. Automatic procedures were also included to aid in the alignment and testing of the system in particular for slit drive calibration, spectrometer calibration and reproducibility tests.

III. ALIGNMENT

The desired high accuracies demand extreme attention to the alignment of the spectrometer components, in particular for the grating, detector and entrance slit. It must be stressed here that, if a parameter cannot be aligned to sufficient accuracy, it must be determined, *i.e* fitted, during the calibration process.

The alignment procedures utilized in this work will now be briefly described. The natural curvature of an emission line was used to aid the grating alignment. The diffraction plane was aligned with respect to the horizontal plane to within 2-3 pixels across the whole visible spectrum by adjusting the lateral grating tilt angle in order to have the center of curvature of emission lines at different wavelengths at the same vertical pixel. Then, exploiting the diffraction pattern of white light through a pinhole at the entrance slit, the detector was aligned with respect to the horizontal plane within one pixel across the whole sensor. The grating tilt angle with respect to the vertical axis was aligned, centering the optical axis (using the center of curvature of emission lines) on the detector to within 8 pixels from the nominal center of the detector. Particular attention was paid to the sine drive setup, the use of a micrometer on the tip of the drive arm of the rotation stage was used to optimize the linearity of the sine drive by adjusting the angle between the drive arm and the grating normal[6].

Chromatic aberration of the lenses caused the full width at half maximum (FWHM) of the emission lines to increase at wavelengths away from where the focus had been optimized. For a system focused in the green (∼5400 Å) the FWHM would become ∼4 times higher in the 7000 Å range of wavelengths. A motorized slit drive was then employed to adjust the position of the slit such that the emission line would always be in focus on the detector. With the use of high precision angle blocks, the slit drive was positioned as close and as parallel to the optical axis as possible. However, even a small deviation of the slit drive from the optical axis would cause a deviation in the grating incident angle and then in the line position on the detector. An automatic procedure was developed to scan the motorized slit, at different wavelengths, around the best focus position and determine, from the horizontal shift on the sensor and the movement along the slit drive, the angle of the slit trajectory with respect to the optical axis. Results, corrected for the anamorphic magnification of the system, at 7 different wavelengths gave consistent values as shown in Fig. 1, determining an angle of the slit drive of 2.482 degrees with respect to the optical axis.

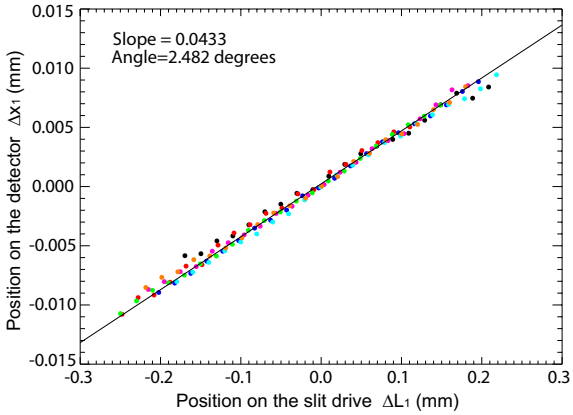

FIG. 1. (Color online) Determination of the angle of the slit drive with respect to the optical axis. The position on the detector as a function of the position along the slit drive is plotted. Different color represent measurements obtained at different wavelengths.

IV. CALIBRATION PROCEDURE

The purpose of the calibration procedure is to fit all parameters in the grating equation to a sufficient precision to determine the wavelength of every emission line across the visible spectrum. In Fig. 1, a schematic drawing of a scanning lens based spectrometer is presented. The grating equation for the spectrometer in Fig. 2 can

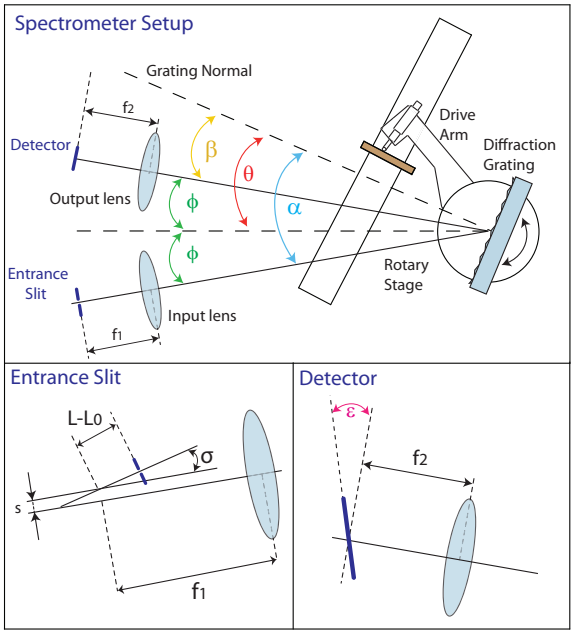

FIG. 2. (Color online) Schematic drawing of the spectrometer setup and angles used in this paper.

be written as:

$$\lambda_{vac} = \frac{dn}{m}\cos\gamma(2\cos\phi\sin\theta + \frac{x_1}{f_1}\cos(\theta+\phi) + \frac{x_2}{f_2}\cos(\theta-\phi) - \frac{x_1^2}{2f_1^2}\sin(\theta+\phi) - \frac{x_2^2}{2f_2^2}\sin(\theta-\phi)), \quad (1)$$

where λ_{vac} is the wavelength in vacuum, d is the grating groove spacing, n is the refraction index of air, m is the spectral order, ϕ is half of the angle between the two lenses, θ is the grating angle, f_1 and f_2 are the focal lengths of the input and output lenses, x_1 and x_2 are the lateral displacements from the optical axis of the entrance slit and detector centers, respectively. γ is the vertical angle with respect to the optical axis, such that $\tan\gamma = y_1/f_1 = y_2/f_2$, y_1 and y_2 being the vertical distances from the optical axis at the slit and detector. This equation was derived, as shown in Ref. 4, by adding small corrections to the incidence and diffraction angles, α and β and rewriting the grating equation in terms of θ and ϕ. Equation 1 is accurate up to second order in the small displacements x_1 and x_2. x_1 can be expressed as in Eq. 2 in order to take into account for the horizontal offset of the input slit and the tilt in the slit drive σ. As in Eq. 3, x_2 can be written to take into account the position of emission lines across the detector and the horizontal tilt in the detector ϵ_x, while the vertical tilt of the detector, ϵ_y, can be included in y_2 as in Eq. 4.

$$\frac{x_1}{f_1} = \frac{s + (L - L_0)\sin\sigma}{f_0 + (L - L_0)\cos\sigma}, \quad (2)$$

$$\frac{x_2}{f_2} = \frac{w_{pixel}(p - p_0)\cos\epsilon_x}{f_0 + w_{pixel}(p - p_0)\sin\epsilon_x}, \quad (3)$$

$$\frac{y_2}{f_2} = \frac{w_{pixel}(l - l_0)\cos\epsilon_y}{f_0 + w_{pixel}(l - l_0)\sin\epsilon_y}. \quad (4)$$

Here w_{pixel} is the pixel width, p and l are the horizontal and vertical pixel positions, p_0 and l_0 are the horizontal and vertical pixel positions of the optical axis, f_0 is the nominal focal length, L is the position across the translation stage of the slit drive, L_0 is the reference position of the translation stage at the optical axis and s is the displacement from the optical axis for the slit at the reference position L_0.

Equations 1-4 will be used to fit all the spectrometer parameters. Using an automated calibration procedure, several spectra N were acquired using a Ne lamp at different grating positions. Particular attention must be given to the choice of the wavelengths to be used for the calibration, being sure to avoid blended lines whose fitting can bring an error in the line position determination. As already pointed out, the detector used in this prototype spectrometer was an 8 bit CMOS detector; the limited dynamic range, the readout noise, maximum exposure level, and fluctuation of the Ne lamp limited the quality of the acquired data. Multiple frames (24) were then acquired at every grating position to improve the photon statistics and average out the fluctuations of the lamp brightness. For every line all the data stacked vertically on the detector were analyzed, a parabola was then fitted to account for the curvature of the emission line and the position of the emission line was determined from the fitted position along the parabola. This procedure helped remove noise and oscillations from the position determination. Atmospheric pressure and temperature were actively recorded at the time of the calibration to correct the refraction index of air[7]. The bulk grating temperature was recorded to adjust for the changes in the grating groove density due to thermal expansion. At this point, the fitted line positions on the 2D detector (independent variable) and the known vacuum wavelengths (dependent variable) were used to fit the adjustable parameters in the grating equation.

The first calibration method simply relies on the positioning of the stepping motor for the grating position. A simplified version of Eq. 1 was employed: only the data at the mid-plane of the detector were analyzed, no slit translation stage was employed and the parameters ϵ_y, s, l_0 and the grating angle offset θ_0 were all fixed. With this procedure, the fitting parameters include θ for N grating positions, ϕ, ϵ_x, f_0 and p_0 for a total of $N+4$ fitting parameters.

The second calibration exploits the availability of a high accuracy measurement of the grating angle. In this way, there is no need to rely on the positioning accuracy of the stepping motor since the actual position can be measured to within 0.075 arcsec. In this calibration method, the sine drive is simply used to approximately position the grating, then the encoder position is read to give the grating angle input to the grating equation. Here the whole grating equation on the 2D detector was used as a fitting function as expressed in Eq. 1. The number of fitted parameters is greatly reduced: ϕ, ϵ_x, ϵ_y, s, f_0, p_0, l_0 and the grating angle offset θ_0 for a total of 8 fitting parameters.

V. RESULTS AND DISCUSSION

Due to issues with signal/noise and line blending only data between between 5800 Å and 7250 Å were used in the fitting of the grating equation, limiting the number of spectra used in the fitting to $N = 27$. The results of the first calibration are reported in Table 1 (first column) and Fig. 3. Overall, the residuals in the wavelength determination have a standard deviation of ∼0.0025 Å. However, an essential part of this calibration is the reproducibility of the stepping motor positioning. A test of reproducibility was conducted by repeatedly switching between two Ne emission lines (∼ 5852 Å and ∼ 6096 Å) 50 times approaching alternatively the lines from a lower and a higher stepping motor position. This test showed that, in order to reduce backlash, lines were to

be approached from higher stepping motor positions and it showed that the actual line position is spread over 2-3 pixels (Fig. 4), which corresponds to an error in the wavelength determination of the order of ∼0.2-0.3 Å (∼10-15 km/s). Additional problems would be expected with the effects of thermal expansion on the driving screw of the stepping motor. This implies that even for calibration accuracies of 0.0025 Å, the accuracy is ultimately limited by the stepping motor resolution and reproducibility to ∼0.2-0.3 Å.

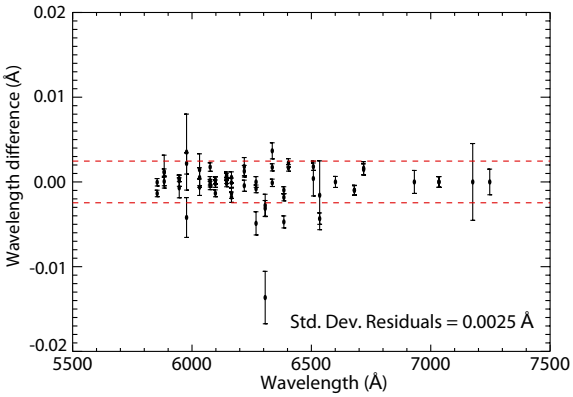

FIG. 3. (Color online) Residuals of the fitting from the first calibration method. The standard deviation (dashed lines) in the residuals is of 0.0025 Å.

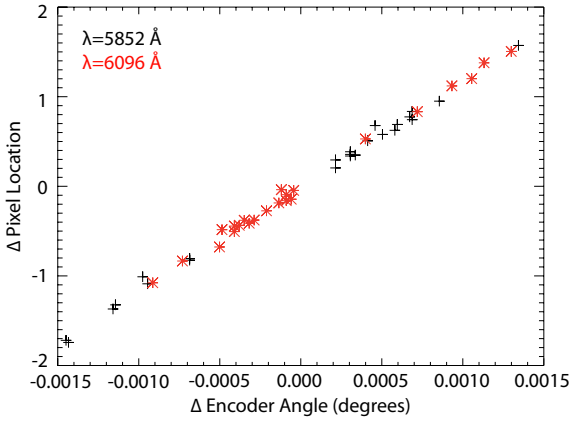

FIG. 4. (Color online) Positioning reproducibility test of the stepping motor. The variation in the position on the detector of two Ne lines (5852 Å black [+], 6096 Å red [∗]) for the same requested motor position is plotted against the change in the grating angle as measured by the encoder.

The results of the second fitting method are reported in Table 1 (second column) and Fig. 5. The use of an independent measurement of the grating angle solved the reproducibility/resolution problems of the stepping motor and temperature effects on the driving screw. This calibration allowed all the wavelengths to be known on the 2D detector to within an accuracy of ∼0.005 Å that corresponds to an error in the velocity of ∼0.2 km/s. It must be stressed here how essential to obtaining high accuracy is good alignment and the ability to preserve the alignment as environmental conditions vary. Further tests to investigate the stability of the alignment over time are envisioned.

TABLE I. Spectrometer fitted parameters

Parameters	Method 1	Error 1	Method 2	Error 2
ϕ (degrees)	10.12869	1.2 e-8	10.18748	4.2e-7
ϵ_x (degrees)	0.75810	3.4e-9	0.90071	6.6e-4
f_0(mm)	196.34423	1.4e-6	196.4579	4.5e-5
p_0 (pixel)	640.02758	7.3e-9	635.01509	8.1e-5
l_0 (pixel)	512	0	519.17959	5.8e-3
ϵ_y (degrees)	0	0	0.150	0.078
s (mm)	0	0	-0.05834	6.0 e-6
θ_0 (degrees)	0	0	0.00554	7.2e-8
θ_i (degrees)	27 values	∼1e-8	–	–

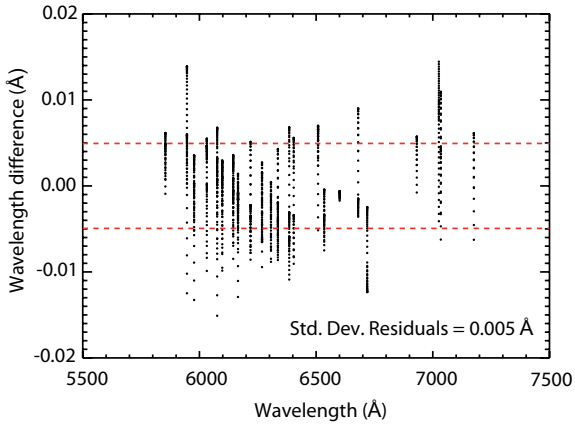

FIG. 5. (Color online) Residuals of the fitting from the second calibration method. The fitting was carried out for unblended lines between 5800 Å and 7250 Å. The standard deviation (dashed lines) in the residuals is of 0.005 Å.

VI. ACKNOWLDGEMENTS

The authors would like to acknowledge the help of W. Boeglin. The support and encouragement of D. W. Johnson and B. C. Stratton is also appreciated. This work was supported by the U.S. DOE under Contract No. DE-AC02-09CH11466.

[1]P. Gohil, K. H. Burrell *et al.*, Rev. Sci. Instrum. **70**, 878 (1999).
[2]K. Ida, S. Kado and Y. Liang, Rev. Sci. Instrum. **71**, 2360 (2000).
[3]J. A. Holy, Appl. Spectrosc. **58**, 1219 (2004).
[4]R. E. Bell and F. Scotti, *High-throughput Accurate-wavelength lens-based Visible Spectrometer*, these conference proceedings.
[5]D. B. Leviton. *U. S. Patent No. 5,965,879*, (12 October 1999).
[6]D. L. Dimock, J. Opt. Soc. Am. **50**, 819 (1960).
[7]P. E. Ciddor, Appl. Opt. **35**, 1566 (1999).

The Princeton Plasma Physics Laboratory is operated
by Princeton University under contract
with the U.S. Department of Energy.

Information Services
Princeton Plasma Physics Laboratory
P.O. Box 451
Princeton, NJ 08543

Phone: 609-243-2245
Fax: 609-243-2751
e-mail: pppl_info@pppl.gov
Internet Address: http://www.pppl.gov